

# Alteration of the Thymic T Cell Repertoire by Rotavirus Infection Is Associated with Delayed Type 1 Diabetes Development in Non-Obese Diabetic Mice

Nicole L. Webster, Christel Zufferey<sup>‡</sup>, Jessica A. Pane, Barbara S. Coulson\*

Department of Microbiology and Immunology, The University of Melbourne, Parkville, Victoria, Australia

## Abstract

Rotaviruses are implicated as a viral trigger for the acceleration of type 1 diabetes in children. Infection of adult non-obese diabetic (NOD) mice with rotavirus strain RRV accelerates diabetes development, whereas RRV infection in infant NOD mice delays diabetes onset. In this study of infant mice, RRV titers and lymphocyte populations in the intestine, mesenteric lymph nodes (MLN) and thymus of NOD mice were compared with those in diabetes-resistant BALB/c and C57BL/6 mice. Enhanced intestinal RRV infection occurred in NOD mice compared with the other mouse strains. This was associated with increases in the frequency of CD8 $\alpha\beta$  TCR $\alpha\beta$  intraepithelial lymphocytes, and their PD-L1 expression. Virus spread to the MLN and T cell numbers there also were greatest in NOD mice. Thymic RRV infection is shown here in all mouse strains, often in combination with alterations in T cell ontogeny. Infection lowered thymocyte numbers in infant NOD and C57BL/6 mice, whereas thymocyte production was unaltered overall in infant BALB/c mice. In the NOD mouse thymus, effector CD4<sup>+</sup> T cell numbers were reduced by infection, whereas regulatory T cell numbers were maintained. It is proposed that maintenance of thymic regulatory T cell numbers may contribute to the increased suppression of inflammatory T cells in response to a strong stimulus observed in pancreatic lymph nodes of adult mice infected as infants. These findings show that rotavirus replication is enhanced in diabetes-prone mice, and provide evidence that thymic T cell alterations may contribute to the delayed diabetes onset following RRV infection.

**Citation:** Webster NL, Zufferey C, Pane JA, Coulson BS (2013) Alteration of the Thymic T Cell Repertoire by Rotavirus Infection Is Associated with Delayed Type 1 Diabetes Development in Non-Obese Diabetic Mice. *PLoS ONE* 8(3): e59182. doi:10.1371/journal.pone.0059182

**Editor:** Cheryl A. Stoddart, University of California, San Francisco, United States of America

**Received:** December 13, 2012; **Accepted:** February 12, 2013; **Published:** March 15, 2013

**Copyright:** © 2013 Webster et al. This is an open-access article distributed under the terms of the Creative Commons Attribution License, which permits unrestricted use, distribution, and reproduction in any medium, provided the original author and source are credited.

**Funding:** This research was supported by the Juvenile Diabetes Research Foundation Award 27-2011-281 (B.S.C.), together with Project Grant 509008 and Senior Research Fellowships 350253 and 628319 (B.S.C.) from the National Health and Medical Research Council of Australia. N.W. was supported by Early Career Researcher Grant 600667 from The University of Melbourne and C.Z. received a Fellowship for Prospective Researchers from the Swiss National Science Foundation (#PBBEP3 128392). The funders had no role in study design, data collection and analysis, decision to publish, or preparation of the manuscript.

**Competing Interests:** The authors have declared that no competing interests exist.

\* E-mail: barbarac@unimelb.edu.au

<sup>‡</sup> Current address: Infectious Diseases and Microbiology, Murdoch Childrens Research Institute, Parkville, Victoria, Australia

## Introduction

Rotaviruses are the major etiologic agents of severe acute infantile gastroenteritis [1]. Environmental factors including viruses are implicated in the rising incidence of type 1 diabetes, an autoimmune disease resulting in T cell-mediated destruction of insulin-producing cells within the pancreas. Diabetes onset is preceded by development of pancreatic islet autoimmunity, including autoantibodies that mark progression towards diabetes [2,3]. Correlations between rotavirus infection and exacerbations in the level of islet autoantibodies in children genetically at-risk of developing diabetes have been observed, suggesting that rotaviruses may play a role in diabetes development [4,5].

Non-obese diabetic NOD/Lt (NOD) mice spontaneously develop diabetes as they age and are a commonly used model for human diabetes [6,7]. Infection of older adult NOD mice with pre-existing islet autoimmunity by monkey rotavirus strain RRV accelerates diabetes onset, whereas RRV infection of infant NOD mice delays diabetes onset [8,9]. RRV is present in the intestine, liver, pancreas, spleen and blood of infant NOD mice, but does not reach the pancreas in the adults. While these findings show the potential for rotaviruses to either accelerate or delay diabetes, the

precise nature of the virus and host factors involved is unclear. Identifying how diabetes can be delayed is necessary to devise strategies for delaying the age of diabetes onset in children and substantially improving their quality of life.

Intestinal T lymphocytes play an important role in the rotavirus-specific immune response. Intraepithelial lymphocytes (IEL) comprise 3–10% of all cells residing within the intestinal epithelium [10]. CD8 $\alpha\beta$  TCR $\alpha\beta$  IEL recognize non-self antigen presented by conventional MHC class I molecules [11], secrete Th1 cytokines (eg. IFN $\gamma$ ) and are cytotoxic during acute viral infection [12,13,14]. Rotavirus-specific CD8<sup>+</sup> T cells present in the IEL compartment and the mesenteric lymph nodes (MLN) at 6 days after infection of adult C57BL/6 mice show direct anti-viral activity for timely resolution of primary infection [15]. CD4<sup>+</sup> T cells are essential for development of the rotavirus-specific IgA response in the intestine [15], and are the only cell type sufficient to confer protection from re-infection [16]. The programmed cell death-ligand 1 (PD-L1) is a costimulatory molecule expressed on a range of cell types including T cells and epithelial cells following stimulation with IFN $\gamma$  [17]. PD-L1 expression is important for T cell activation, cytokine production and virus-specific T cell responses [18,19]. During coxsackievirus B3 or lymphocytic

choriomeningitis virus infection, PD-L1 expressed by lymphocytes inhibits diabetogenic CD8<sup>+</sup> T cell expansion in NOD mice, delaying diabetes development [20]. It is possible that PD-L1 also may play a role in the delayed diabetes onset in NOD mice following rotavirus infection. However, the dynamics of PD-L1 expression on CD8<sup>+</sup> IEL during the acute phase of rotavirus infection has not been investigated.

Type 1 diabetes reflects a loss of tolerance to self-antigen. In central tolerance, potentially autoreactive lymphocytes emerging in the thymus are eliminated. This process is incomplete so additional peripheral tolerance mechanisms exist, including immune response suppression by regulatory T cells (Treg) via TGFβ and IL-10 production. Virus infection of the thymus has the potential to affect tolerance and diabetes development [21,22,23]. Like RRV, reovirus infection delays diabetes onset in infant NOD mice. Proposed mechanisms for the reovirus-mediated delay include infection of the thymus resulting in loss of autoreactive T cells and passive tolerance [24,25]. Although untested to date, it is plausible that rotavirus might delay murine diabetes through thymic infection and effects on the T cell repertoire, particularly as infectious RRV is present in the thymus of infant rats [26].

The main aim of the current study was to investigate the effect of RRV infection on T lymphocytes in the intestine, lymph nodes and thymus of infant NOD, C57BL/6 and BALB/c mice. It was demonstrated that intestinal RRV infection is enhanced in NOD mice over the other strains, in association with increases in CD8αβ TCRαβ IEL frequency and T cell numbers in MLN. Thymic RRV infection, shown here for the first time in mice, was associated with altered T cell ontogeny. NOD mice alone showed an increased ratio of CD4<sup>+</sup> Treg to CD4<sup>+</sup> T effector cells (Teff) produced in the thymus following RRV infection. This may prolong suppression of inflammatory T cell responses in the pancreatic lymph node (PLN) and contribute to the delayed diabetes onset.

## Materials and Methods

### Mice

Mice obtained from the Animal Resource Centre, Western Australia were bred and housed in the Biological Research Facility of the Department of Microbiology and Immunology at the University of Melbourne in individually ventilated micro-isolator cages under specific pathogen free conditions as previously described [8].

### Ethics statement

Principles of laboratory animal care' (NIH publication no. 85–23) and the 'Australian Code of Practice for the Care and Use of Animals for Scientific Purposes (2004)' were followed. All procedures were conducted in accordance with protocols approved by the Animal Ethics Committee of The University of Melbourne (ID 1011742).

### Mouse inoculation with RRV and diabetes monitoring

Monkey rotavirus RRV was cultivated in MA104 cells (American Type Culture Collection), purified by glycerol gradient ultracentrifugation, and titrated for infectivity as before [27,28]. Five day-old mice were inoculated by oral feeding with 10 μl of either 50 mM Tris HCl pH 7.4 containing 150 mM NaCl and 5 mM CaCl<sub>2</sub> (TSC; mock-inoculated controls) or TSC containing 6 × 10<sup>6</sup> fluorescent forming cell units (FCFU) of RRV, as described previously [8]. In indicated experiments, female NOD mice (aged-matched to females given RRV as infants where indicated), were infected at 12 weeks of age by oral gavage with 2 × 10<sup>6</sup> FCFU of

RRV in 200 μl of TSC, as before [8,9]. Mice reaching 6 weeks of age were monitored weekly for diabetes onset by blood or urinary glucose testing, as described previously [8,9].

### Assay for antibodies to rotavirus

Titers of rotavirus antibodies in mouse sera were determined by EIA with RRV antigen on the solid phase, as previously described [8]. Seroconversion was defined as a four-fold increase in titer. All dams were negative for serum antibodies to RRV prior to experimentation. All infant mice infected with RRV that reached 14 days of age were tested at this time and shown to seroconvert to RRV.

### Detection of infectious RRV and determination of RRV titer

The procedures for collection and processing of tissues have been described previously [8] apart from the thymus and MLN, which were prepared as a 10% (wt/vol) homogenate in TSC. Infectious RRV was detected by culture amplification in MA104 cells for 72 h followed by antigen capture EIA, as before [29,30]. Virus titers were determined by MA104 cell culture and indirect immunofluorescent staining, as described previously [28,29].

### Cell isolation from thymus, MLN, PLN and spleen

Tissues were mechanically disrupted between glass slides. Released cells were filtered through 70 μm nylon mesh and washed with either RPMI containing 10% (vol/vol) fetal bovine serum (FBS; RF10) for cell culture or with FACS buffer (1% (vol/vol) FBS in Ca<sup>2+</sup>- and Mg<sup>2+</sup>-free PBS with 0.01% (wt/vol) NaN<sub>3</sub>) for antibody staining and flow cytometric analysis. Cell counts were determined with a hemocytometer.

### IEL isolation

This method was adapted from [31]. Briefly, 0.5 cm to 1 cm long pieces of small intestine were stirred in Ca<sup>2+</sup>- and Mg<sup>2+</sup>-free HBSS containing 10 mM HEPES, 2% (vol/vol) FBS, 0.5 mM EDTA and 2 mM dithiothreitol at 37°C for 30 min, followed by two further incubations in the absence of dithiothreitol. Detached cells were counted prior to flow cytometric analysis.

### Enzyme-linked immunospot assay (ELISPOT)

MLN cells (2 × 10<sup>5</sup>/well) cultured in RF10 containing 10% (vol/vol) FBS and IL-2 at 40 U/ml were stimulated at 20 μg/ml with a peptide corresponding to amino acids 5 to 13 of RRV VP7 (GenScript) [32], or 50 ng/ml PMA and 500 ng/ml ionomycin as a positive control, for 48 h. Cells responding to the peptide were identified with mouse IFNγ ELISPOT and 2-amino-9-ethylcarbazole (AEC) kits (BD). Stained cells were viewed and counted by microscopy.

### Flow cytometric analysis of isolated cells

Cells (1 × 10<sup>6</sup>) were resuspended in FACS buffer for antibody staining. IEL were stained with conjugated antibodies as follows: anti-CD3 (500A2)-Alexa700, anti-CD4 (RM4-5)-Pacific Blue, anti-CD8α (53-6.7)-PerCP, anti PD-L1 (MIH5)-phycoerythrin (PE) (all from BD), anti-T cell receptor (TCR) β-chain (H57-597)-PE-Cy7 (Biolegend, San Diego, CA), anti-TCRγδ (GL-3)-allophycocyanin (APC) and anti-CD8β (ebioH35-17.2)-biotin (eBioscience). Streptavidin APC-Alexa 750 (Invitrogen) was used as secondary antibody. Thymus, spleen and lymph node cells were stained with anti-CD3, anti-CD8α, anti-CD4, anti-CD25 (PC61)-APC and anti-Foxp3 (FJK-16 s)-PE. The Foxp3 staining buffer set (eBioscience) was used for intracellular staining. IFNγ intracellular

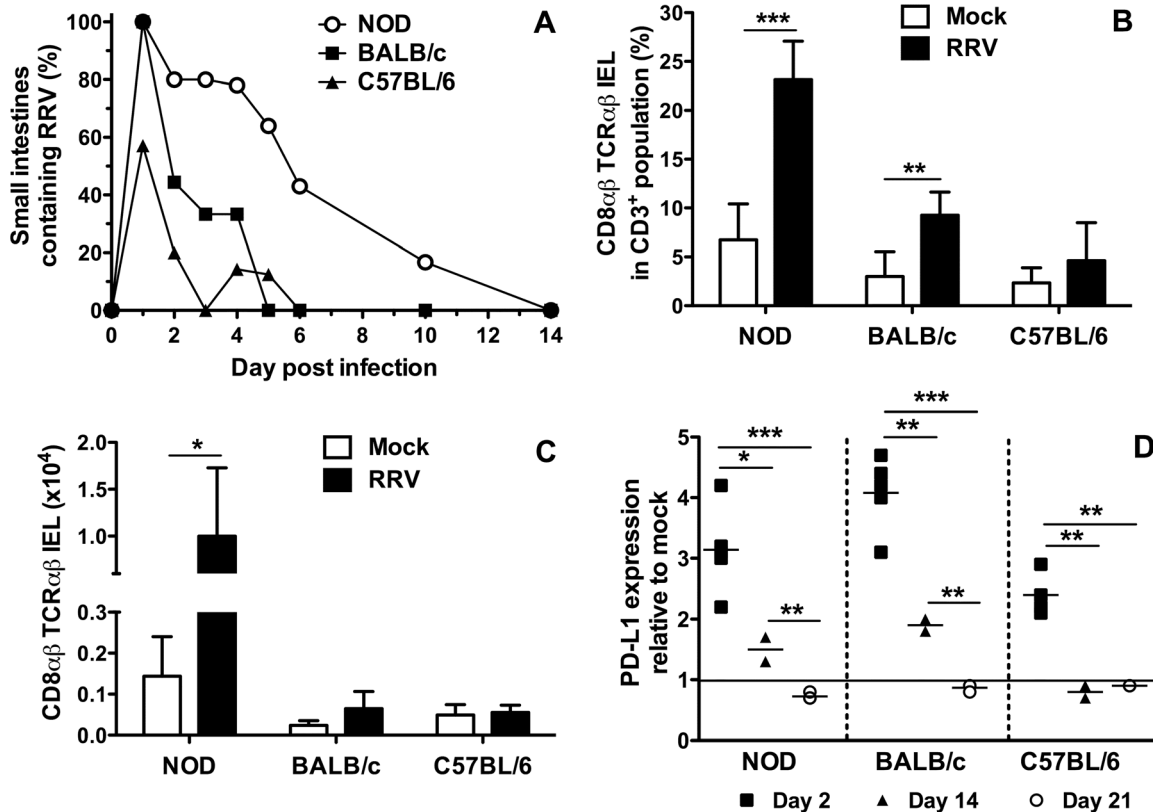


**Figure 1. RRV replication and IEL responses in the small intestine of RRV-infected infant mice.** A, Proportion of intestines containing infectious RRV following inoculation of 5 day-old NOD, BALB/c and C57BL/6 mice. Infectious RRV was detected by 72 h co-culture with MA104 cells followed by EIA. At each day post infection, intestines from 5 to 6 NOD mice were analysed. On days 1, 2, 3, 4, 5, 6, 10 and 14 post infection, intestines from 8, 9, 6, 9, 6, 8, 5 and 6 BALB/c mice and 7, 5, 7, 7, 8, 9, 7, and 6 C57BL/6 mice were assayed, respectively. B, Frequency and C, absolute numbers of CD8 $\alpha\beta$  TCR $\alpha\beta$  IEL on day 2 post mock- or RRV infection. To obtain sufficient cells, 4 to 6 separate cell pools were analysed for each inoculum. Each pool was produced from 2 to 5 (NOD), 2 to 3 (BALB/c) or 3 to 5 (C57BL/6) mice. Cell numbers from pools were normalized to represent cells obtained from a single mouse. D, PD-L1 expression by CD8 $\alpha\beta$  TCR $\alpha\beta$  IEL in RRV-infected mice on days 2, 14 and 21 after infection. Data are expressed as the ratio of PD-L1 expression on cells from RRV-infected mice to the mean PD-L1 expression of mock-infected mice. The numbers of mice analysed and usage of cell pools for day 2 studies were as described for B and C. For days 14 and 21 post infection, each data point represents a pool of cells from 2 (NOD), 3 to 4 (BALB/c) or 2 to 3 (C57BL/6) mice. \*  $p < 0.05$ ; \*\*  $p < 0.01$ ; \*\*\*  $p < 0.001$ . Bar = mean. doi:10.1371/journal.pone.0059182.g001

staining was performed using anti-IFN $\gamma$  (XMG1.2)-FITC and Cytotfix/Cytoperm Plus kit (BD). Acquisition of at least  $5 \times 10^5$  cells was performed on the LSR II (BD) and data analysed with FlowJo 8.7.1 (Tree Star). The absolute number of each cell subset was calculated using the frequency of the subset of interest obtained by flow cytometry and the total number of cells determined by hemocytometer counts.

### Immunohistochemistry and histology

Thymuses were fixed in 2% (vol/vol) paraformaldehyde and embedded in paraffin. Sections (4  $\mu$ m) were cut, deparaffinised, blocked with 10% (vol/vol) goat serum in PBS for 30 min and reacted for 30 min with either rabbit anti-RRV antiserum or normal rabbit serum (rotavirus antibody-negative), each diluted 1 in 500 in PBS containing 0.5% (vol/vol) FBS. Endogenous peroxidase activity was blocked with 1 part 3% (vol/vol) H $_2$ O $_2$  solution in 4 parts methanol for 20 min. Bound antibody was detected with HRP-conjugated goat anti-rabbit antibody (Millipore) and SIGMAFAST<sup>TM</sup>. The location of RRV-positive cells in serial sections counterstained with hematoxylin was identified by microscopy, and images collected using Leica LAS software v 3.8.

### PLN cell proliferation

Isolated cells were serially diluted from  $4 \times 10^5$  cells/well in U-bottomed 96 well plates (Nunc) and cultured with anti-CD3 (2  $\mu$ g/ml; BD), anti-CD28 (1  $\mu$ g/ml; BD) and IL-2 (20 U/ml; Peprotech) in RF10. Controls comprised cells alone and cells with IL-2 alone. Cultures were incubated for 72 h at 37°C with 5% (vol/vol) CO $_2$ . Cell proliferation was assessed by addition of  $^3$ H-thymidine at 1  $\mu$ Ci/well for the final 24 h of incubation. Cells were collected onto glass fibre filters using an automated cell harvester (Skatron Instruments) and  $\beta$ -emission recorded by a liquid scintillation counter (Packard Bell) in counts/min.

**Statistical analysis.** Student's t-test, with Welch's correction as appropriate, was used to assess statistical significance, which was set at the 95% level. On graphs, error bars indicate the SD unless otherwise indicated.

### Results

#### NOD mice showed the greatest extent of intestinal RRV replication

RRV-infected infant NOD mice exhibit diarrhoea for 2 to 5 days, and intestinal RRV presence for up to 9 days [8]. We found here that diarrhoea following oral RRV infection of infant BALB/

c and C57BL/6 mice lasted for 5 to 8 days and 1 day, respectively. At day 1 post infection all intestines from NOD (n = 6) and BALB/c mice (n = 8) contained infectious RRV, whereas only 4/7 C57BL/6 were RRV-positive (Fig. 1A). By day 3 post infection, 4/5 NOD, 2/6 BALB/c and 0/7 C57BL/6 mouse intestines remained infected. NOD mice showed the longest period of RRV presence intestinally. The reciprocal geometric mean titers of infectious RRV intestinally in NOD and BALB/c mice did not differ significantly (p>0.05), but both were significantly increased over those in C57BL/6 mice at day 1 post-infection (Table 1; p≤0.0044). NOD mice showed the greatest proportion of mice with detectable infectious RRV at all days post infection except day 1, when BALB/c mice showed an equal rate (Fig. 1A). Although intestinal RRV was detected over a similar period (4 to 5 days) in BALB/c and C57BL/6 mice, a lesser proportion of C57BL/6 than BALB/c mice showed intestinal RRV replication (Fig. 1A). The proportion of mice showing infectious RRV intestinally and their RRV titers were associated with the extent of diarrhoea observed, as BALB/c and NOD mice showed more protracted diarrhoea, greater infection rates and higher titers than C57BL/6 mice.

**Intestinal IEL responses to RRV infection in NOD, BALB/c and C57BL/6 mice**

The effect of RRV infection on intestinal CD8<sup>+</sup> T cells in infant mice was determined by isolation and characterisation of intestinal IEL at 2, 5, 11, 14, 21 and 35 days after RRV or mock inoculation. The frequency of CD8αβ TCRαβ IEL at day 2 was significantly increased over controls in RRV-infected NOD and BALB/c mice, but not C57BL/6 mice (p = 0.023, p = 0.0001 and p>0.05, respectively; Fig 1B). CD8αβ TCRαβ IEL numbers were significantly increased in RRV-infected NOD mice (p = 0.029), but not BALB/c or C57BL/6 mice (p>0.05; Fig 1C). RRV-infected NOD mice showed fewer CD8αβ TCRαβ IEL (mean ± SD = 1.0 ± 0.01 × 10<sup>4</sup> cells) than mock-infected mice (mean ± SD = 2.0 ± 0.20 × 10<sup>4</sup> cells; p = 0.02) at day 14 post-infection (data not shown). Aside from this, no change in CD8αβ TCRαβ IEL frequency or numbers was observed in any mouse strain later than 2 days post-infection (data not shown).

PD-L1 expression on CD8αβ TCRαβ IEL of RRV-infected infant mice increased by a mean of 2.4- to 4.0-fold relative to control mice for all mouse strains at day 2 post infection (Fig. 1D; 0.0001 ≤ p ≤ 0.0030). By day 14 post infection, PD-L1 expression on these IEL was similar to control levels in C57BL/6 mice, but remained elevated by a mean of 1.5- and 1.9-fold in NOD and BALB/c mice, respectively (0.0012 ≤ p ≤ 0.0038). PD-L1 expression returned to control levels in all mice by day 21.

These data showed an association between the unaltered frequency of CD8αβ TCRαβ IEL in infant C57BL/6 mice and their low rates of gastrointestinal symptoms and infection. Similarly, the prolonged elevation of PD-L1 on the CD8αβ TCRαβ IEL of NOD and BALB/c mice related to the increased severity and duration of their diarrhoea, and elevated virus replication. In contrast, we found that RRV infection of 12 week-old NOD mice did not significantly alter the frequency, numbers and PD-L1 expression of CD8αβ TCRαβ IEL at days 2, 5 10 and 21 post infection (p>0.05; Fig. S1), consistent with the lack of diarrhoea and reduced intestinal RRV replication in these older mice [9].

**RRV titers in the MLN were highest in NOD mice**

Infectious RRV is present in the pancreas, liver, spleen and blood of RRV-infected infant NOD mice, but other extraintestinal sites have not been analysed [8]. We examined the MLN for the

**Table 1. RRV titers in homogenates of small intestines and MLN from RRV-infected infant BALB/c, NOD and C57BL/6 mice.**

Day post infection	Proportion of organs in the given mouse strain from which a virus titer was obtained, and the virus titer											
	Small intestine				MLN							
	NOD		BALB/c		C57BL/6		NOD		BALB/c		C57BL/6	
	% of mice <sup>1</sup>	Virus titer <sup>2</sup>	% of mice	Virus titer	% of mice	Virus titer	% of mice	Virus titer	% of mice	Virus titer	% of mice	Virus titer
1	100 (6/6)	3,300 (510–20,000)	100 (8/8)	1,100 (240–2,600)	29 (2/7)	410 (120–1,400)	0 (0/6)	NA <sup>3</sup>	0 (0/8)	NA	0 (0/7)	NA
2	80 (4/5)	450 (240–960)	33 (3/9)	550 (240–960)	20 (1/5)	120	80 (4/5)	65 (23–390)	0 (0/9)	NA	0 (0/5)	NA
3	60 (3/5)	750 (480–1,200)	17 (1/6)	480	0 (0/7)	NA	40 (2/5)	85 (45–160)	33 (2/6)	45 (45–45)	0 (0/7)	NA
4	ND <sup>4</sup>	ND	22 (2/9)	960 (480–1,900)	14 (1/7)	480	100 (5/5)	1,300 (230–4,700)	22 (2/9)	220 (160–300)	43 (3/7)	96 (24–900)
5	ND	ND	0 (0/6)	NA	0 (0/8)	NA	80 (4/5)	1,600 (450–11,000)	33 (2/6)	500 (160–1,600)	25 (2/8)	7 (4–12)
6	ND	ND	0 (0/8)	NA	0 (0/9)	NA	0 (0/5)	NA	63 (5/8)	58 (12–180)	0 (0/9)	NA

<sup>1</sup>Percentage (no. giving a virus titer/no. collected) of mouse organs where an infectious virus titer could be determined. All organs where a titer was measurable also showed infectious virus by co-culture (Fig. 1A, 2A).

<sup>2</sup>Reciprocal geometric mean titer (range) of RRV in FCFU/organ. No range is given when only a single sample yielded a virus titer.

<sup>3</sup>Not applicable. No infectious RRV was detected by titration.

<sup>4</sup>Not done. In previous studies our group detected virus in 67% of intestines from RRV-infected NOD mice on days 4 and 5, and 40% on day 6 [8].

doi:10.1371/journal.pone.0059182.t001

presence of infectious RRV. Although a minority of MLN from all mouse strains contained infectious RRV at day 1 after infection (Fig. 2A), titres could not be determined due to low levels (Table 1). In NOD mice, most or all MLN on days 2 to 5 post infection contained RRV, with titers maximal at days 4 and 5 (Fig. 2A, Table 1). RRV spread to MLN was delayed in BALB/c mice, peaking at day 6 post infection when 6/8 MLN contained infectious RRV. This is consistent with previous studies where virus was detected by PCR [33]. Similarly, RRV titers were maximal on days 4 to 6 (Table 1). Infectious RRV was detected in 1/7 to 2/8 C57BL/6 mice on days 1 to 6 post infection, except for day 4 when the infection rate and virus titers peaked at 4/7 mice. MLN RRV titers in C57BL/6 mice remained low throughout the study (Table 1). C57BL/6 mice showed the least proportion of MLN with detectable virus titers, providing evidence that virus replicates to lower titers in these mice. RRV titers in the MLN were significantly greater in NOD than BALB/c and C57BL/6 mice on days 4 to 5 after infection ( $p=0.035$  and  $p=0.040$ , respectively; Table 1).

### RRV infection increased T cell numbers in the MLN at day 2 after infection in NOD mice

The effect on RRV infection on MLN T cell numbers was determined.  $CD4^+$  T cell (Fig. 2B) and  $CD8\alpha\beta$  TCR $\alpha\beta$  T cell (Fig. 2C) numbers increased over controls in the MLN of NOD mice at day 2 post infection ( $p=0.0017$  and  $p=0.0025$ , respectively). However, in BALB/c and C57BL/6 mice these MLN cell numbers were similar between mock- and RRV-infected

mice ( $p>0.05$ ; Fig 2B, 2C). As the peak of RRV replication in MLN occurred at day 4 to 5 post infection, T cell numbers also were determined in RRV-infected mice at day 6 post infection. T cell numbers were similar in NOD and BALB/c mice, but were lower in C57BL/6 mice (Fig 2D).  $CD4^+$  rather than  $CD8^+$  T cell numbers were lower in RRV-infected C57BL/6 mice compared with the other mouse strains. The respective frequencies of  $CD8^+$  T cells expressing IFN $\gamma$  at day 6 post infection (means $\pm$ SD in NOD, BALB/c and C56BL/6 mice of  $6.1\pm 4.8\%$ ,  $5.8\pm 2.3\%$  and  $9.3\pm 5.5\%$ , respectively) did not differ ( $p>0.05$ ; data not shown). Additionally, RRV-specific cells detected by IFN $\gamma$  ELISPOT were rare in all three strains of mice, with 1 in  $10^4$  mononuclear cells from MLN of RRV-infected mice stimulated with RRV VP7 5–13 peptide [32] secreting IFN $\gamma$  (data not shown). This rate is similar to that seen previously with this peptide in BALB/c mice [34]. Overall,  $CD4^+$  and  $CD8^+$  T cell numbers were increased by RRV infection in NOD mice on days 2 and 6 post infection, BALB/c mice showed evidence of increased numbers on day 6, and T cell numbers were unaltered in C57BL/6 mice. No difference in the extent of  $CD8^+$  T cell activation between mouse strains was observed.

### Infectious RRV was present in the thymus of NOD, BALB/c and C57BL/6 mice during the first 5 days after infection

RRV was found above to alter T cell numbers in the intestine and MLN, and can spread to other organs [8]. As the thymus is the source of the T cell repertoire, it was examined for the presence of RRV. The proportion of RRV-infected NOD mouse

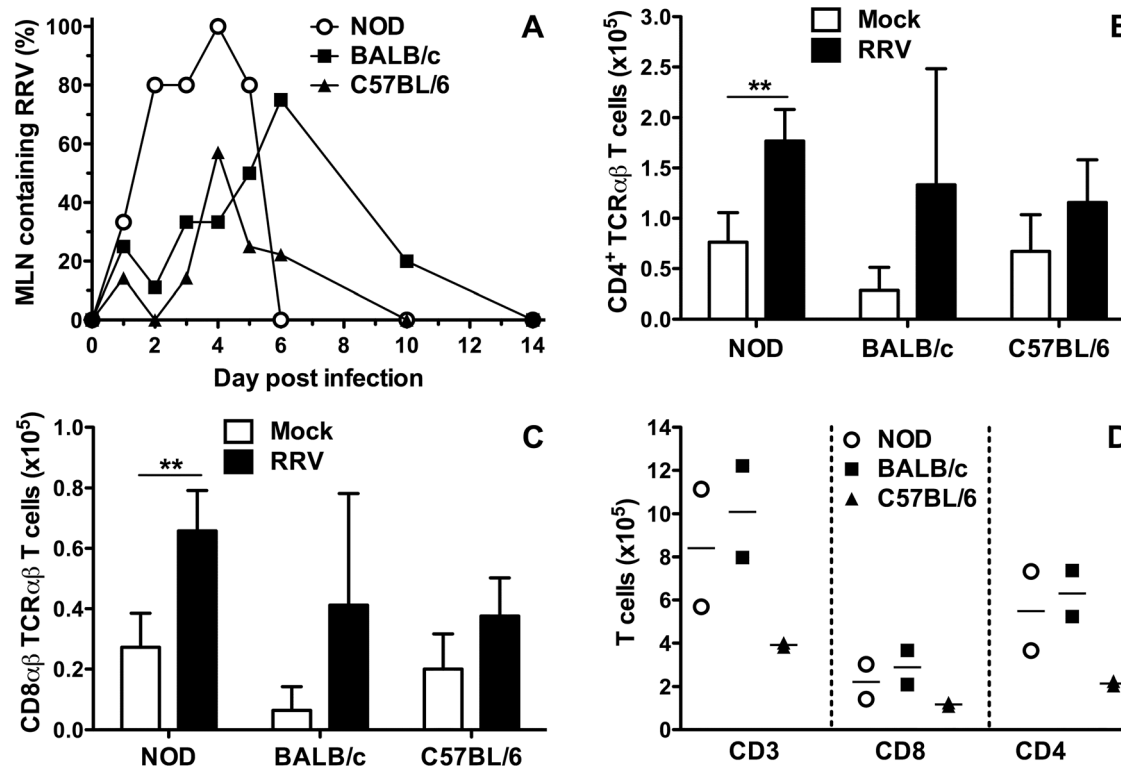


**Figure 2. RRV replication and T cell subsets in the MLN of RRV-infected infant mice.** A, Proportion of MLN containing infectious RRV. The numbers of mice analysed on each day are given in the Legend to Fig. 1A. Absolute numbers of  $CD4^+$  TCR $\alpha\beta$  T cells (B) and  $CD8\alpha\beta$  TCR $\alpha\beta$  T cells (C) at day 2 post infection are shown. To obtain sufficient cells, 4 to 5 separate cell pools were analysed for each inoculum. Each pool was produced from 4 to 5 (NOD), 3 to 4 (BALB/c) or 3 to 5 (C57BL/6) mice. Cell numbers from pools were normalized to represent cells obtained from a single mouse. D, Absolute numbers of  $CD3^+$ ,  $CD8^+$  and  $CD4^+$  T cells from RRV-infected mice at day 6 post infection. Each data point represents a pool of cells from 4 (NOD), 3 (BALB/c) or 3 to 4 (C57BL/6) mice. \*  $p<0.05$ ; \*\*  $p<0.01$ . Bar = mean. doi:10.1371/journal.pone.0059182.g002

thymuses peaked at day 2 post infection (6/8) with titers ranging from 10 to 1500 FCFU/thymus (Fig. 3, Table 2). Biphasic intestinal rotavirus infection can occur in infant BALB/c mice [35], although this was not evident in our study (Fig. 1A, 2A). However, BALB/c mice showed biphasic thymus infection, with 6/8 thymuses containing infectious virus at 1 day post infection in the initial peak and a second peak when 5/9 thymuses were infected at day 4 (Fig. 3). RRV titers (FCFU/thymus) ranged from 380 to 11,000 on day 1 and 1,300 to 15,000 on day 4 post infection (Table 2). C57BL/6 infection was maximal day 1 post infection with 5/7 thymuses positive, containing titres of 17 to 3,200 FCFU. By day 2, RRV levels in the 2/8 positive thymuses were too low to be determined by titration (Table 2). Thymic RRV infection was restricted to 5 days for all mice, as it was undetectable on days 6, 10 and 14 post infection (Fig. 3 and data not shown).

### Nature and location of RRV-infected cells in the thymus

In sections of thymus obtained at the peak time of infectious RRV detection from NOD (day 2 post infection), BALB/c (days 1 and 4) and C57BL/6 (day 1) mice, RRV-infected cells were detected in the cortex and the adipose tissue under the capsule. Their morphology indicated that they were macrophages (Fig. 4). Numbers of infected macrophages were highest in BALB/c mice, with 1 to 4 seen per section in the cortex and adipose tissue on both days (Fig. 4A to 4E). Infected macrophages were less often observed in the cortex of NOD and C57BL/6 mice, and adipose tissue of C57BL/6 mice, and were rare in NOD adipose tissue (Fig. 4F). As positive and negative selection occur in the cortex, RRV-infected macrophages potentially could affect both these processes.

### RRV infection alters the thymic T cell repertoire

The effect of RRV infection on thymocyte populations was determined after virus clearance. At day 7 post infection for all three mouse strains, no significant alterations in thymocyte numbers between mock- and RRV-infected mice were detected ( $p > 0.05$ ; data not shown). At day 14 (Fig. 5A) the total number of thymocytes isolated from RRV-infected NOD and BALB/c mice was unaltered compared to age-matched, mock-infected controls ( $p > 0.05$ ; Fig. 5A). In contrast, thymocyte numbers in C57BL/6 mice were significantly decreased over controls ( $p = 0.04$ ; Fig. 5A).

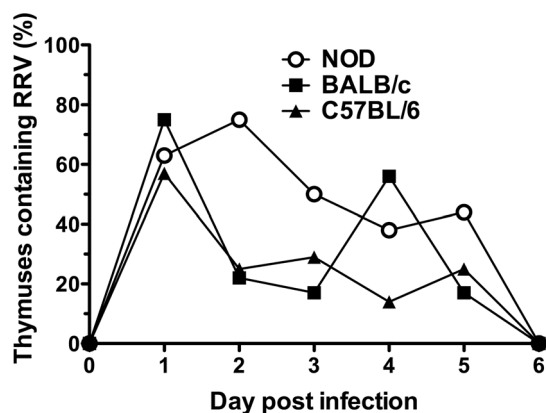


**Figure 3. Thymic infection by RRV.** On days 1, 2, 3, 4, 5 and 6 post infection, thymuses were assayed for the presence of infectious RRV by co-culture from 8, 8, 8, 8, 9 and 5 NOD mice, 8, 9, 6, 9, 6 and 8 BALB/c mice and 7, 8, 7, 7, 6 and 9 C57BL/6 mice, respectively. doi:10.1371/journal.pone.0059182.g003

During thymic T cell development, immature cells expressing neither CD4 nor CD8 (double negative; DN) evolve to express both CD4 and CD8 (double positive; DP) and undergo both positive and negative selection. The small minority of cells expressing a T cell receptor that binds MHC or peptide with at least a weak affinity are positively selected. DP cells with a high affinity for self-peptide or MHC undergo negative selection through apoptosis. DP cells with intermediate affinity can be converted into Treg ( $CD4^+CD25^+Foxp3^+$ ), and those with low affinity for self-antigen become Teff. At the end of the final, single positive (SP) stage of maturation, cells expressing either CD4 or CD8 located in the medulla are ready for release [36].

These stages of thymocyte development were analysed by enumeration of CD4 SP, CD8 SP, DN and DP cells at day 14 post infection (Fig. 5B). The numbers and frequency of cells at each stage were not significantly altered by RRV infection of infant NOD and BALB/c mice ( $p > 0.05$ ; Fig. 5C, 5D and data not shown), consistent with their unchanged total thymocyte numbers (Fig. 5A). In C57BL/6 mice (Fig. 5E), the proportion of DN cells was significantly decreased by RRV infection ( $p = 0.04$ ), a trend for an increased proportion of DP cells was evident ( $p = 0.05$ ) and CD8 SP cell proportions were unaltered ( $p > 0.05$ ). CD4 SP proportion and numbers were not reduced significantly by infection in these C57BL/6 mice ( $p = 0.14$ ; Fig. 5E). However, their CD8 SP, DP and DN cell numbers were significantly decreased ( $p \leq 0.04$ ; Fig. 5F), reflecting the decrease in total thymocyte numbers due to RRV infection (Fig. 5A).

At day 21 post infection, total thymocyte numbers in NOD mice were significantly reduced over controls ( $p = 0.020$ ; Fig. 6A). The DP cell frequency decreased, whereas CD8 SP and DN cell frequency increased ( $p \leq 0.0019$ ), and the CD4 SP frequency was unaltered ( $p = 0.14$ , Fig. 6B). RRV infection significantly decreased the numbers of CD4 SP, DP and DN thymocytes in NOD mice at day 21 post infection ( $p \leq 0.020$ ; Fig. 6C), and CD8 SP cells showed a possible trend for reduced numbers ( $p = 0.064$ ; Fig. 6C). In contrast to NOD mice, total thymocyte numbers in BALB/c and C57BL/6 mice were similar to those of age-matched, mock-infected controls ( $p > 0.11$ , Fig. 6A). As expected from these data, the thymocyte frequency and number for each developmental stage were similar between infected and control BALB/c or C56BL/6 mice at day 21 (data not shown).

### RRV infection decreased T cell numbers in the thymus of NOD mice, while Treg numbers were preserved

T cells ( $CD3^+$ ) in the CD4 SP population can be further divided into Treg that express CD25 and Foxp3, and Teff that lack Foxp3 expression. It was shown above that total thymocyte or CD4 SP cell numbers in infant NOD and C57BL/6 mice were reduced by RRV infection at days 14 or 21 after infection, the age when the thymus reaches its plateau in Treg production in infant mice [37]. Repeated transfer of Treg into infant NOD mice has been shown to delay their diabetes onset [38]. The effect of RRV infection on thymic production of Treg and Teff therefore was investigated. As expected from the unaltered CD4 SP cell number and frequency at day 14 after RRV infection in NOD mice (Fig. 5D), Treg and Teff numbers at this time also were unaffected by RRV infection (Fig. 7A). However, at day 21 post infection  $CD4^+$  Teff cell numbers were significantly reduced over controls in RRV-infected NOD mice ( $p = 0.022$ ; Fig. 7A), whereas Treg numbers were unaltered ( $p = 0.079$ ; Fig. 7A). Consistent with their unchanged thymocyte levels on days 14 and 21 post infection (Fig. 5, 6), Treg and Teff numbers and frequency were unaltered in BALB/c mice at these times ( $p > 0.05$ ; data not shown). Treg and Teff numbers were unchanged at day 21 after RRV infection in C57BL/6 mice

**Table 2.** Titers of RRV in thymus homogenates from infant BALB/c, NOD and C57BL/6 mice.

Day post infection	Proportion of thymuses in the given mouse strain from which a virus titer was obtained, and the virus titer					
	NOD		BALB/c		C57BL/6	
	% of mice <sup>1</sup>	Virus titer <sup>2</sup>	% of mice	Virus titer	% of mice	Virus titer
1	25 (2/8)	2,100 (340–13,000)	75 (6/8)	2,400 (380–11,000)	71 (5/7)	170 (17–3,200)
2	75 (6/8)	390 (100–1,500)	22 (2/9)	500 (190–1,300)	0 (0/8)	NA <sup>3</sup>
3	38 (3/8)	410 (68–1,200)	17 (1/6)	190	29 (2/7)	880 (510–1,500)
4	25 (2/8)	110 (71–1,700)	56 (5/9)	3,500 (1,300–15,000)	14 (1/7)	1,500
5	0 (0/9)	NA	17 (1/6)	3,000	33 (2/6)	260 (170–410)

<sup>1</sup>Percentage (no. giving a virus titer/no. collected) of mouse thymuses where an infectious virus titer could be determined. All organs where a titer was measurable also showed infectious virus by co-culture (Fig. 3).

<sup>2</sup>Reciprocal geometric mean titer (range) of RRV in FCFU/thymus. No range is given when only a single thymus yielded a virus titer.

<sup>3</sup>NA, not applicable. The infectious RRV level was below the limit of detection by titration.

doi:10.1371/journal.pone.0059182.t002

(Fig. 7B). In contrast, there was a trend for reduced Treg and Teff numbers at day 14 ( $p = 0.05$  and  $p = 0.06$ , respectively; Fig. 7B). In order to determine if RRV infection induced similar effects on Treg and Teff cells in the periphery to those seen in the thymus, splenocytes at day 14 and PLN cells at day 21 after inoculation also were evaluated. Treg and  $CD3^+CD4^+$  T cell numbers in RRV-infected NOD mouse spleens were similar to those in mock-infected mice ( $p > 0.05$ ; Fig. 7C), reflecting the thymus data. In

C57BL/6 mice, similar reductions to those found in the thymus also were present in the spleen ( $p = 0.008$  and  $p = 0.06$ , respectively; Fig. 7C). Neither NOD nor C57BL/6 mice showed altered Treg or  $CD3^+CD4^+$  T cell numbers in the PLN at day 21 following RRV infection ( $p > 0.05$ ; Fig. 7D). Overall, preservation of thymic Treg during loss of thymic Teff  $CD4^+$  T cells at day 21 after NOD mouse infection resulted in an increased thymic Treg:Teff ratio. This alteration was not detected simultaneously in

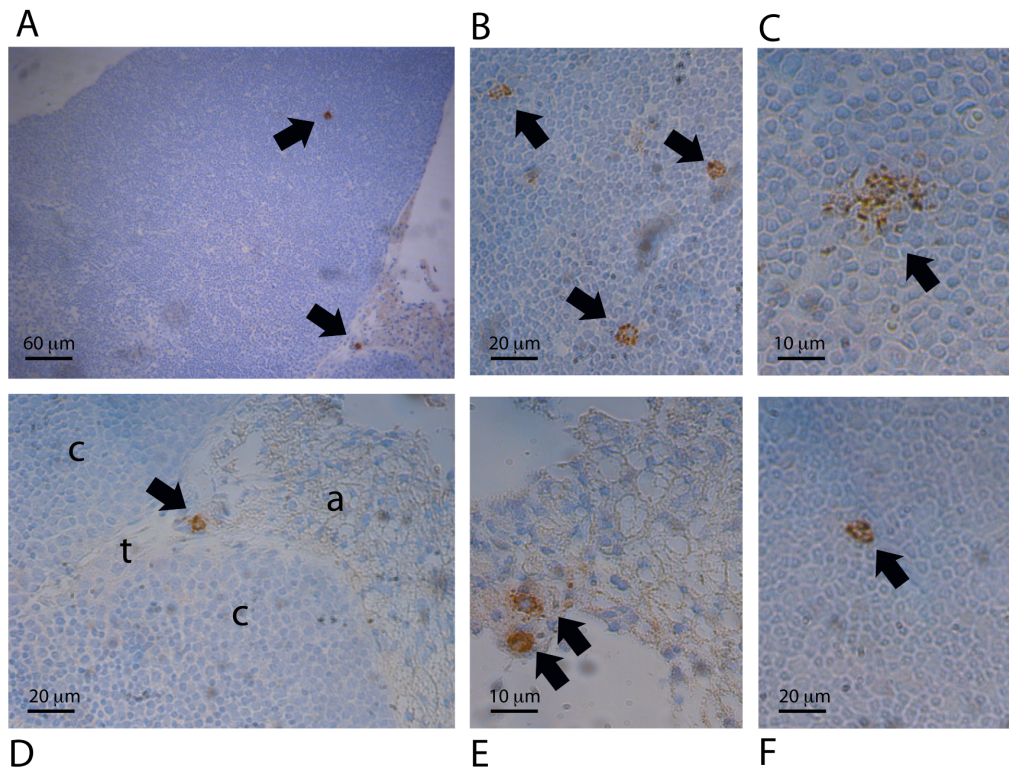


**Figure 4. Identification of macrophages as the RRV-infected cells in the thymus, and their location.** Thymus sections from 8 infants of each mouse strain were examined at the peak of thymic infection by immunohistochemistry. A, Representative section showing infected macrophages in the cortex and adipose tissue ( $\times 100$ ). B, Three infected macrophages in the cortex ( $\times 300$ ). C, Infected macrophage in the cortex ( $\times 600$ ). D, Higher magnification ( $\times 300$ ) image of an infected macrophage from A in the adipose tissue (a) near the trabeculae (t) and cortex region (c). E, Two infected macrophages in the adipose tissue under the thymus capsule ( $\times 600$ ). F, Rare infected macrophage in the cortex region of the NOD thymus ( $\times 300$ ). All images except F are from thymuses of BALB/c mice at 4 days post infection. No cells positive for RRV were seen in matching sections stained with the negative control antibody, or in thymus sections from mock-infected mice of the same strain at the same day post-infection. doi:10.1371/journal.pone.0059182.g004

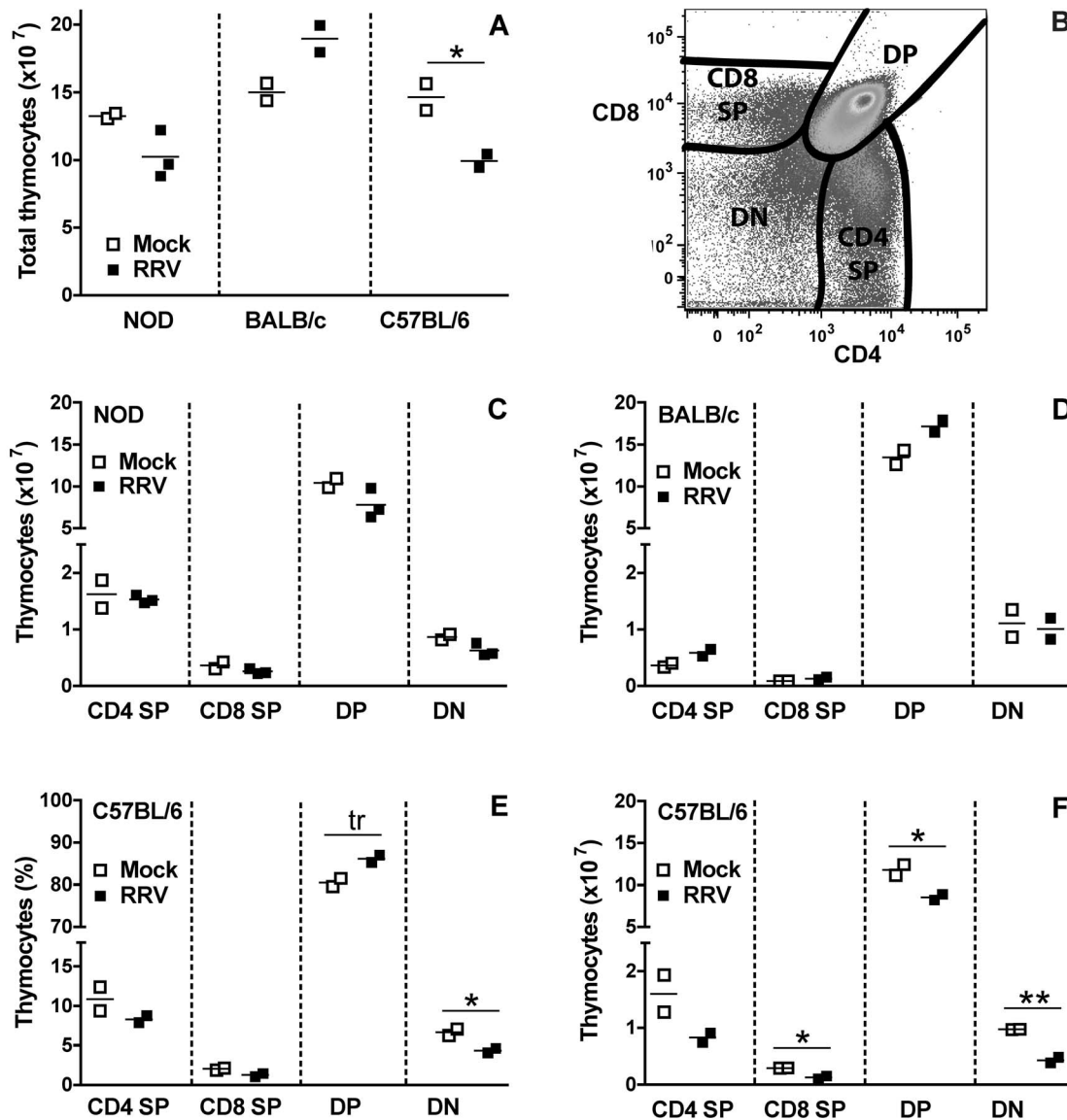


**Figure 5. Effect of RRV on T cell populations in the thymus of mice at 14 days post infection.** A, Total number of thymocytes obtained. B, Flow cytometry gating strategy for identification of the frequency of the CD4 SP, CD8 SP, DP and DN thymocyte subsets. The absolute number of each thymocyte subset in NOD and BALB/c analysed in A is shown in C and D, respectively. The frequency (E) and absolute number (F) of thymocyte subsets in C57BL/6 mice analysed in A was determined by flow cytometry gating and cell counts, respectively. For A to F, each data point indicates results from a pool of cells from 2 to 4 mice, normalized to represent cells obtained/mouse. Cell pooling was necessary to obtain sufficient cells for analysis. Bar = mean. \*  $0.02 \leq p \leq 0.04$ ; \*\*  $p = 0.008$ ; tr = trend,  $p = 0.05$ . doi:10.1371/journal.pone.0059182.g005

the PLN. This increased thymic Treg:Teff ratio may favor prolonged Treg suppression of self-reactive T cells once these Treg establish in the periphery.

#### Adult NOD mice infected as infants produced PLN cells with reduced proliferative capacity in response to T cell stimulation

NOD mice have reduced Treg numbers [38] and the suppressive ability of their Treg wanes with age [39]. Reduced Teff suppression occurs in part through reduced Treg function and also by an increasing resistance of NOD Teff to suppression mediated by Treg [39,40,41]. NOD mice aged 10 weeks show extensive pancreatic infiltration by T and B lymphocytes, NK cells, dendritic cells and macrophages, which precedes diabetes

onset from approx. 12 weeks of age [42]. The PLN is the priming site for T cells that migrate into the pancreas [43,44].

In order to determine the effect of RRV infection in infant mice on their T cell function as adults, the proliferative response by PLN cells was examined. Age-matched female NOD mice were mock- or RRV-infected as infants (5 days old) or adults (aged 12 weeks) and their PLN cell responses compared when they reached either 17 or 20 weeks of age. Regular testing showed that these mice were non-diabetic. The entire PLN cell population was used to best represent the lymphocytes present. T cell numbers in this population were similar between mock and RRV-infected mice, so results were not confounded by variation in input T cell number (data not shown). PLN cells from NOD mice that were RRV-infected as an infant showed significantly less proliferation in

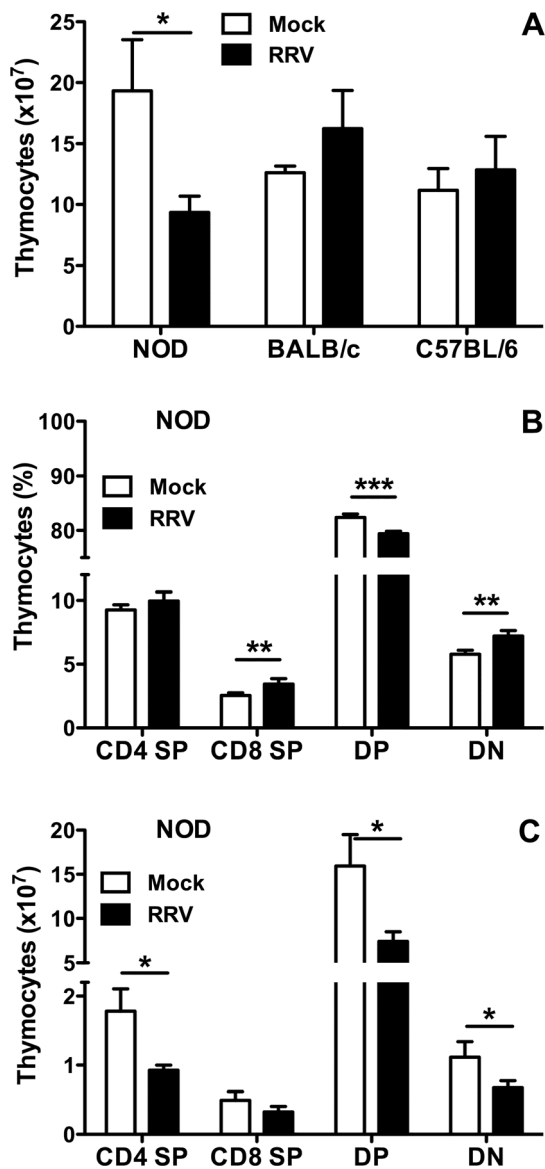


**Figure 6. Effect of RRV on T cell populations in the thymus at 21 days post infection.** A, Total number of thymocytes recovered from mock- and RRV-infected mice. For each inoculum, 4 (NOD), 3 (BALB/c) and 2 (C57BL/6) individual pools of cells were analysed. Each cell pool was produced from 2 (NOD), 2 to 3 (BALB/c) or 3 to 4 (C57BL/6) mice. Cell numbers from pools were normalized to represent cells obtained/mouse. The frequency (B) and absolute number (C) of thymocytes in the CD4 SP, CD8 SP, DP and DN thymocyte populations (defined in Fig. 5B) of the NOD mice described in A was determined by flow cytometry gating and cell counts, respectively. \*  $p < 0.05$ ; \*\*  $p < 0.01$ ; \*\*\*  $p < 0.001$ . doi:10.1371/journal.pone.0059182.g006

response to strong T cell stimulus at 17 weeks of age than mock-infected mice ( $p = 0.035$ ; Fig. 8). In contrast, PLN cells from mice infected with RRV as adults were significantly more proliferative than those from mice infected as infants ( $P = 0.025$ ; Fig. 8), in line with the accelerated diabetes onset observed in RRV-infected adult mice [9]. By 20 weeks of age, PLN T cell proliferation in mice infected as infants was similar between RRV-infected and control mice (data not shown), consistent with the previous demonstration that RRV infection as an infant delays but does not completely prevent diabetes [8]. It is possible that the waning in

ability of Treg to suppress Teff that occurs in naïve NOD mice is delayed but not abolished by RRV infection. Overall, infection of infant NOD mice with RRV transiently decreased the proliferative ability of T cells in response to a strong T cell stimulus, most likely as the result of increased Treg function or decreased Teff resistance to Treg suppression.

## Discussion

Following RRV rotavirus infection as an infant, it is shown here that virus replication in the intestine and MLN is greater in diabetes-prone NOD mice than diabetes-resistant mouse strains. Furthermore, the extent of diarrhoea varies between mouse strains and is related to the degree of RRV replication in the intestine, MLN and thymus. Higher gastroenteritis rates also correlate with increased numbers of CD8<sup>+</sup> IEL showing prolonged elevations in PD-L1 expression. We have demonstrated for the first time that RRV spreads to the mouse thymus and can alter T cell development. Although thymocyte production is reduced at 3 weeks after RRV infection in NOD mice, thymic Treg numbers are maintained. Furthermore, at 17 weeks of age in NOD mice given RRV as infants, PLN T cells show decreased proliferative ability in response to a strong stimulus. It is proposed that the maintenance of thymic Treg numbers at the time of reduced T cell production leads to this decreased T cell proliferative response in the PLN, which could contribute to the delayed diabetes onset in NOD mice following RRV infection as an infant.

IEL also accumulate during murine viral infection with reovirus [45], and intestinal T cell numbers are increased in rotavirus-infected calves [46]. RRV infection induces a rapid expansion of CD8 $\alpha\beta$  TCR $\alpha\beta$  IEL in infant NOD mice (Fig. 1A, 1B) but not in adult NOD (Fig. S1) or C57BL/6 mice [47]. RRV infection had no effect on CD8<sup>+</sup> TCR $\gamma\delta$  IEL, which increased as a proportion of total T cells from  $19 \pm 4\%$  on day 14 post infection to  $47 \pm 2\%$  on day 21 and  $59 \pm 1\%$  on day 35 in both mock- and RRV-infected NOD mice (C. Zufferey and B. S. Coulson, unpublished data). These results confirm previous findings that the TCR $\gamma\delta$  IEL frequency in mice reaches  $\sim 50\%$  by 20 days of age, and are consistent with the lack of effect of reovirus infection on TCR $\gamma\delta$  IEL frequency compared to control mice [48,49]. The low level of RRV replication in infant C57BL/6 mice may explain their unaltered numbers of CD8 $\alpha\beta$  TCR $\alpha\beta$  IEL and rapid decrease in PD-L1 expression intestinally. The extensive RRV replication by day 1 post infection in NOD and BALB/c mice results in higher numbers of CD8 $\alpha\beta$  TCR $\alpha\beta$  IEL to fight infection. Endothelial MHC class I levels are higher in NOD than BALB/c mice, influencing T cell proliferation, adhesion and transmigration of CD8<sup>+</sup> T cells in NOD mice [50]. The elevated CD8 $\alpha\beta$  TCR $\alpha\beta$  T cell numbers in the IEL compartment of NOD over BALB/c mice (Fig. 1C, 1D) could result from increased RRV antigen presentation on MHC class I.

The increased frequency of CD8 $\alpha\beta$  TCR $\alpha\beta$  IEL and their extended PD-L1 expression is evident in BALB/c and NOD but not C57BL/6 mice, and might relate to the degree of virus replication. The increased PD-L1 expression at 2 days post infection suggests a role for PD-L1 in an enhanced immune response for clearance of rotavirus infection. PD-L1 interaction with PD-1 plays an important role in preventing autoimmune disease by inducing T cell anergy and tolerance [17]. However, in pathogen-specific T cell responses, PD-L1 is involved in T cell activation, proliferation and cytokine production [18,19,51]. In line with this latter PD-L1 role, our results show that PD-L1 expression correlates with the extent of intestinal rotavirus replication in all mouse strains. PD-L1 expression on CD8<sup>+</sup> T

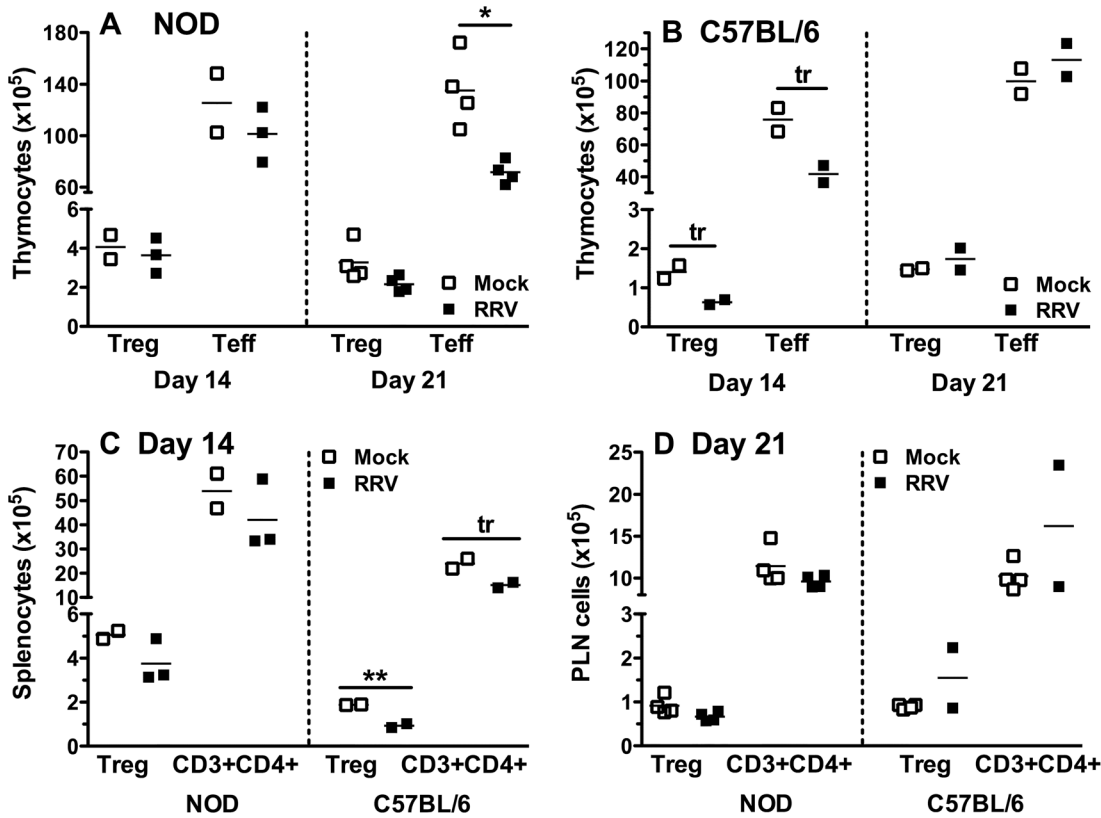


**Figure 7. Thymic Treg numbers were maintained in NOD mice on days 14 and 21 after infection.** Absolute numbers of thymic Treg (CD3<sup>+</sup>CD4<sup>+</sup>CD25<sup>+</sup>Foxp3<sup>+</sup>) and Teff (CD3<sup>+</sup>CD4<sup>+</sup>Foxp3<sup>-</sup>) cells in NOD (A) and C57BL/6 (B) mice on days 14 and 21 post infection. Each data point indicates results from a pool of cells from 2 to 4 mice, normalized to represent cells obtained from a single mouse. C, Decreases in total CD4<sup>+</sup> T cell (CD3<sup>+</sup>CD4<sup>+</sup>) numbers, and in the Treg subset (CD3<sup>+</sup>CD4<sup>+</sup>CD25<sup>+</sup>Foxp3<sup>+</sup>) in the spleen (C) and PLN (D) of RRV-infected NOD and C57BL/6 mice compared with controls at days 14 (C) and 21 (D) post infection. Each data point represents a pool of cells from 4 to 5 mice, normalized to represent cells/mouse. Greater numbers of PLN cell pools than thymocyte and splenocyte pools were analysed from C57BL/6 mice, due to PLN availability from other studies. Bar = mean. \* p = 0.02; \*\* p = 0.008; tr = trend, 0.05 ≤ p ≤ 0.06. doi:10.1371/journal.pone.0059182.g007

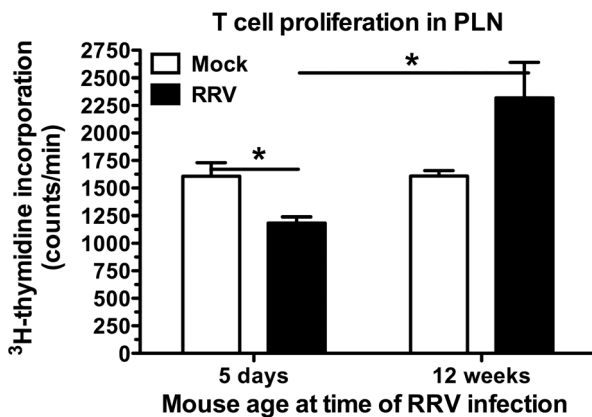


**Figure 8. Reduced T cell proliferation by PLN cells from adult NOD mice infected as infants.** PLN cells from groups of age-matched mice, which had been mock- or RRV-infected either as infants (5 days of age) or adults (12 weeks of age), were harvested at 17 weeks of age. Equivalent numbers of cells from mice in each group were stimulated with antibodies to CD3 and CD28. T cell proliferation was measured by <sup>3</sup>H-thymidine incorporation (counts/min). Data for 4 × 10<sup>5</sup> cells/well are shown. A pool of cells from 4 (infected as infant) or 5 (infected as adult) mice was analysed in triplicate for each inoculum. \* p < 0.05. doi:10.1371/journal.pone.0059182.g008

cells in other tissues may prove to be a useful marker of rotavirus infection.

Our detection of RRV in thymic macrophages extends the earlier identification of macrophages as the likely main RRV source in the infant NOD mouse pancreas, and supports the proposal that macrophages disseminate rotavirus infection [8]. Altered thymic T cell development following infection by any virus that delays diabetes has not been reported to date. However, in an adult SJL/J mouse model of virus-induced diabetes, coxsackievirus B4 infection of the thymus, pancreas and other organs was associated with an increased DN thymocyte frequency but unaltered overall thymocyte numbers at 21 days post infection [52]. In fetal thymic organ cultures from CD-1 mice, coxsackievirus B4 increased the frequency of DN, CD4 SP and CD8 SP cells and decreased DP cells [53]. Thymic RRV infection in NOD mice also was associated with increased proportions of CD8 SP and DN, and decreased DP cells, although CD4 SP cell proportions were unaltered. However, total thymocyte numbers were decreased due to reductions in CD4 SP, DP and DN cells, in contrast to the coxsackievirus B4 studies [52,53]. Thus, reduced overall thymocyte numbers, combined with maintenance of CD4 SP cells, might contribute to the RRV-mediated diabetes delay. However, the effect of RRV on thymocytes is mouse strain-dependent, with most subsets and total cell numbers decreased in C57BL/6 mice, but no effect in BALB/c mice. The differing

thymic effects of coxsackievirus and rotavirus in diabetes mouse models may relate to their contrasting effects on diabetes and the mouse strain utilized.

NOD mice show a normal ability to generate and maintain Treg in the thymus [54]. However, diabetes develops as Treg become functionally defective in the periphery with age, and self-reactive T<sub>H</sub>17 increasingly develop resistance to Treg-mediated suppression [39,40,41]. We found that RRV-infected NOD mice maintain thymic Treg production at day 21 post infection when CD4<sup>+</sup> T<sub>H</sub>17 and other thymocyte subsets are reduced. At this time, the number and proliferative function of T cells in the PLN and MLN of mock- and RRV-infected NOD mice are similar (Fig. 7D and data not shown), as expected once infection is cleared and homeostasis has been restored. PLN T cells from NOD mice aged 17 weeks, which had been RRV-infected as infants, are less proliferative to a strong T cell stimulus than cells from age-matched, mock-infected mice. It is proposed that RRV infection of infant NOD mice may prolong Treg immunosuppression, which could contribute to their delayed diabetes onset. A lowering of T<sub>H</sub>17 resistance to Treg-mediated regulation [40,41] during RRV infection also may be a factor in this reduced T cell proliferation that occurs following a strong stimulus.

The wide range of immunological defects in NOD mice includes resistance to thymic deletion and increased production of autoimmune T cells [6,7]. For example, DP thymocytes from NOD mice have a lower activation threshold than those of C57BL/6 and BALB/c mice [36]. Although we have associated Treg maintenance and decreased T cell proliferation after a strong T cell stimulus with the delayed diabetes after RRV infection, it is also possible that rotavirus infection of the NOD thymus induces stronger activation of the normally weakly activated self-T cells,

leading to their deletion and contributing to the delayed diabetes onset. Further studies now are warranted to address the effects of rotavirus infection on thymic T cell activation, and the role of immunosuppression by Treg in the delayed diabetes mediated by RRV.

## Supporting Information

**Figure S1 Intestinal IEL responses following RRV infection of 12 week-old female NOD mice.** A, Frequency and B, absolute numbers of CD8 $\alpha\beta$  TCR $\alpha\beta$  IEL in the intestine at days 2 to 21 after mock- or RRV infection. C, PD-L1 expression by CD8 $\alpha\beta$  TCR $\alpha\beta$  IEL in the intestines of RRV-infected mice at days 2, 5 and 21 post infection. Data are expressed as the ratio of PD-L1 expression on cells from RRV-infected mice to the mean PD-L1 expression of mock-infected mice. Each data point represents a single mouse. Bar = mean. (TIFF)

## Acknowledgments

We are most grateful to David Taylor, Rhiannon Hall, Emma Rooney and other staff members of the Biological Research Facility at the University of Melbourne for their excellent mouse breeding and animal husbandry.

## Author Contributions

Conceived and designed the experiments: BSC NLW CZ. Performed the experiments: NLW CZ JAP. Analyzed the data: BSC NLW CZ JAP. Contributed reagents/materials/analysis tools: BSC NLW CZ JAP. Wrote the paper: NLW CZ BSC JAP.

## References

- Glass RI, Parashar UD, Bresee JS, Turcios R, Fischer TK, et al. (2006) Rotavirus vaccines: current prospects and future challenges. *Lancet* 368: 323–332.
- Maclaren N, Lan M, Coutant R, Schatz D, Silverstein J, et al. (1999) Only multiple autoantibodies to islet cells (ICA), insulin, GAD65, IA-2 and IA-2beta predict immune-mediated (Type 1) diabetes in relatives. *J Autoimmun* 12: 279–287.
- Barker JM, Barriga KJ, Yu L, Miao D, Erlich HA, et al. (2004) Prediction of autoantibody positivity and progression to type 1 diabetes: Diabetes Autoimmunity Study in the Young (DAISY). *J Clin Endocrinol Metab* 89: 3896–3902.
- Honeyman MC, Coulson BS, Stone NL, Gellert SA, Goldwater PN, et al. (2000) Association between rotavirus infection and pancreatic islet autoimmunity in children at risk of developing type 1 diabetes. *Diabetes* 49: 1319–1324.
- Lehuen A, Diana J, Zaccane P, Cooke A (2010) Immune cell crosstalk in type 1 diabetes. *Nat Rev Immunol* 10: 501–513.
- Hanafusa T, Miyagawa J, Nakajima H, Tomita K, Kuwajima M, et al. (1994) The NOD mouse. *Diabetes Res Clin Pract* 24 Suppl: S307–311.
- Solomon M, Sarvetnick N (2004) The pathogenesis of diabetes in the NOD mouse. *Adv Immunol* 84: 239–264.
- Graham KL, O'Donnell JA, Tan Y, Sanders N, Carrington EM, et al. (2007) Rotavirus infection of infant and young adult nonobese diabetic mice involves extraintestinal spread and delays diabetes onset. *J Virol* 81: 6446–6458.
- Graham KL, Sanders N, Tan Y, Allison J, Kay TW, et al. (2008) Rotavirus infection accelerates type 1 diabetes in mice with established insulinitis. *J Virol* 82: 6139–6149.
- Beagley KW, Fujihashi K, Lagoo AS, Lagoo-Deenadaylan S, Black CA, et al. (1995) Differences in intraepithelial lymphocyte T cell subsets isolated from murine small versus large intestine. *J Immunol* 154: 5611–5619.
- Johansson-Lindbom B, Agace WW (2007) Generation of gut-homing T cells and their localization to the small intestinal mucosa. *Immunol Rev* 215: 226–242.
- Fujisura Y, Kawaguchi M, Kondo Y, Obana S, Yamamoto H, et al. (1996) Development of CD8 alpha alpha+ intestinal intraepithelial T cells in beta 2-microglobulin- and/or TAP1-deficient mice. *J Immunol* 156: 2710–2715.
- Lundqvist C, Melgar S, Yeung MM, Hammarstrom S, Hammarstrom ML (1996) Intraepithelial lymphocytes in human gut have lytic potential and a cytokine profile that suggest T helper 1 and cytotoxic functions. *J Immunol* 157: 1926–1934.
- Muller S, Buhler-Jungo M, Mueller C (2000) Intestinal intraepithelial lymphocytes exert potent protective cytotoxic activity during an acute virus infection. *J Immunol* 164: 1986–1994.
- Franco MA, Greenberg HB (1997) Immunity to rotavirus in T cell deficient mice. *Virology* 238: 169–179.
- McNeal MM, VanCott JL, Choi AH, Basu M, Flint JA, et al. (2002) CD4 T cells are the only lymphocytes needed to protect mice against rotavirus shedding after intranasal immunization with a chimeric VP6 protein and the adjuvant LT(R192G). *J Virol* 76: 560–568.
- Greenwald RJ, Freeman CJ, Sharpe AH (2005) The B7 family revisited. *Annu Rev Immunol* 23: 515–548.
- Dong H, Zhu G, Tamada K, Chen L (1999) B7-H1, a third member of the B7 family, co-stimulates T-cell proliferation and interleukin-10 secretion. *Nat Med* 5: 1365–1369.
- Talay O, Shen CH, Chen L, Chen J (2009) B7-H1 (PD-L1) on T cells is required for T-cell-mediated conditioning of dendritic cell maturation. *Proc Natl Acad Sci U S A* 106: 2741–2746.
- Filippi CM, Estes EA, Oldham JE, von Herrath MG (2009) Immunoregulatory mechanisms triggered by viral infections protect from type 1 diabetes in mice. *J Clin Invest* 119: 1515–1523.
- Jaidane H, Sane F, Hiar R, Goffard A, Gharbi J, et al. (2012) Immunology in the clinic review series; focus on type 1 diabetes and viruses: enterovirus, thymus and type 1 diabetes pathogenesis. *Clin Exp Immunol* 168: 39–46.
- Jeker LT, Bour-Jordan H, Bluestone JA (2012) Breakdown in peripheral tolerance in type 1 diabetes in mice and humans. *Cold Spring Harb Perspect Med* 2: a007807.
- Jaidane H, Caloone D, Lobert PE, Sane F, Dardenne O, et al. (2012) Persistent infection of thymic epithelial cells with coxsackievirus B4 results in decreased expression of type 2 insulin-like growth factor. *J Virol* 86: 11151–11162.
- Onodera T, Taniguchi T, Tsuda T, Yoshihara K, Shimizu S, et al. (1991) Thymic atrophy in type 2 reovirus infected mice: immunosuppression and effects of thymic hormone. *Thymus* 18: 95–109.
- Wetzel JD, Barton ES, Chappell JD, Baer GS, Mochow-Grundny M, et al. (2006) Reovirus delays diabetes onset but does not prevent insulinitis in nonobese diabetic mice. *J Virol* 80: 3078–3082.
- Crawford SE, Patel DG, Cheng E, Berkova Z, Hyser JM, et al. (2006) Rotavirus viremia and extraintestinal viral infection in the neonatal rat model. *J Virol* 80: 4820–4832.
- Coulson BS, Fowler KJ, Bishop RF, Cotton RG (1985) Neutralizing monoclonal antibodies to human rotavirus and indications of antigenic drift among strains from neonates. *J Virol* 54: 14–20.

28. Coulson BS, Kirkwood C (1991) Relation of VP7 amino acid sequence to monoclonal antibody neutralization of rotavirus and rotavirus monotype. *J Virol* 65: 5968–5974.
29. Hewish MJ, Takada Y, Coulson BS (2000) Integrins alpha2beta1 and alpha4beta1 can mediate SA11 rotavirus attachment and entry into cells. *J Virol* 74: 228–236.
30. Londrigan SL, Hewish MJ, Thomson MJ, Sanders GM, Mustafa H, et al. (2000) Growth of rotaviruses in continuous human and monkey cell lines that vary in their expression of integrins. *J Gen Virol* 81: 2203–2213.
31. Binda E, Erhart D, Schenk M, Zufferey C, Renzulli P, et al. (2009) Quantitative isolation of mouse and human intestinal intraepithelial lymphocytes by elutriation centrifugation. *J Immunol Methods* 344: 26–34.
32. Buesa J, Raga JV, Colomina J, de Souza CO, Munoz C, et al. (1999) Rotavirus-specific cytotoxic T lymphocytes recognize overlapping epitopes in the amino-terminal region of the VP7 glycoprotein. *Virology* 257: 424–437.
33. Blutt SE, Fenaux M, Warfield KL, Greenberg HB, Conner ME (2006) Active viremia in rotavirus-infected mice. *J Virol* 80: 6702–6705.
34. Jaimes MC, Feng N, Greenberg HB (2005) Characterization of homologous and heterologous rotavirus-specific T-cell responses in infant and adult mice. *J Virol* 79: 4568–4579.
35. Burns JW, Krishnaney AA, Vo PT, Rouse RV, Anderson LJ, et al. (1995) Analyses of homologous rotavirus infection in the mouse model. *Virology* 207: 143–153.
36. Kwon H, Jun HS, Yang Y, Mora C, Mariathasan S, et al. (2005) Development of autoreactive diabetogenic T cells in the thymus of NOD mice. *J Autoimmun* 24: 11–23.
37. Fontenot JD, Dooley JL, Farr AG, Rudensky AY (2005) Developmental regulation of Foxp3 expression during ontogeny. *J Exp Med* 202: 901–906.
38. Wu AJ, Hua H, Munson SH, McDevitt HO (2002) Tumor necrosis factor- $\alpha$  regulation of CD4+CD25+ T cell levels in NOD mice. *Proc Natl Acad Sci U S A* 99: 12287–12292.
39. Tritt M, Sgouroudis E, d'Hennezel E, Albanese A, Piccirillo CA (2008) Functional waning of naturally occurring CD4+ regulatory T-cells contributes to the onset of autoimmune diabetes. *Diabetes* 57: 113–123.
40. You S, Belghith M, Cobbold S, Alyanakian MA, Gouarin C, et al. (2005) Autoimmune diabetes onset results from qualitative rather than quantitative age-dependent changes in pathogenic T-cells. *Diabetes* 54: 1415–1422.
41. D'Alise AM, Auyeung V, Feuerer M, Nishio J, Fontenot J, et al. (2008) The defect in T-cell regulation in NOD mice is an effect on the T-cell effectors. *Proc Natl Acad Sci U S A* 105: 19857–19862.
42. Kikutani H, Makino S (1992) The murine autoimmune diabetes model: NOD and related strains. *Adv Immunol* 51: 285–322.
43. Gagnerault MC, Luan JJ, Lotton C, Lepault F (2002) Pancreatic lymph nodes are required for priming of  $\beta$  cell reactive T cells in NOD mice. *J Exp Med* 196: 369–377.
44. Hoglund P, Mintern J, Waltzinger C, Heath W, Benoist C, et al. (1999) Initiation of autoimmune diabetes by developmentally regulated presentation of islet cell antigens in the pancreatic lymph nodes. *J Exp Med* 189: 331–339.
45. Cuff CF, Cebra CK, Rubin DH, Cebra JJ (1993) Developmental relationship between cytotoxic alpha/beta T cell receptor-positive intraepithelial lymphocytes and Peyer's patch lymphocytes. *Eur J Immunol* 23: 1333–1339.
46. Parsons KR, Hall GA, Bridger JC, Cook RS (1993) Number and distribution of T lymphocytes in the small intestinal mucosa of calves inoculated with rotavirus. *Vet Immunol Immunopathol* 39: 355–364.
47. Offit PA, Cunningham SL, Dudzik KI (1991) Memory and distribution of virus-specific cytotoxic T lymphocytes (CTLs) and CTL precursors after rotavirus infection. *J Virol* 65: 1318–1324.
48. Bharhani MS, Grewal JS, Peppler R, Enockson C, London L, et al. (2007) Comprehensive phenotypic analysis of the gut intra-epithelial lymphocyte compartment: perturbations induced by acute reovirus 1/L infection of the gastrointestinal tract. *Int Immunol* 19: 567–579.
49. Steege JC, Buurman WA, Forget PP (1997) The neonatal development of intraepithelial and lamina propria lymphocytes in the murine small intestine. *Dev Immunol* 5: 121–128.
50. Lozanoska-Ochser B, Peakman M (2009) Level of major histocompatibility complex class I expression on endothelium in non-obese diabetic mice influences CD8 T cell adhesion and migration. *Clin Exp Immunol* 157: 119–127.
51. Rowe JH, Johanns TM, Ertelt JM, Way SS (2008) PDL-1 blockade impedes T cell expansion and protective immunity primed by attenuated *Listeria monocytogenes*. *J Immunol* 180: 7553–7557.
52. Chatterjee NK, Hou J, Dockstader P, Charbonneau T (1992) Coxsackievirus B4 infection alters thymic, splenic, and peripheral lymphocyte repertoire preceding onset of hyperglycemia in mice. *J Med Virol* 38: 124–131.
53. Brilot F, Jaidane H, Geenen V, Hober D (2008) Coxsackievirus B4 infection of murine foetal thymus organ cultures. *J Med Virol* 80: 659–666.
54. Feuerer M, Jiang W, Holler PD, Satpathy A, Campbell C, et al. (2007) Enhanced thymic selection of FoxP3+ regulatory T cells in the NOD mouse model of autoimmune diabetes. *Proc Natl Acad Sci U S A* 104: 18181–18186.